Less is More
or
Back to Kohn-Sham

Samuel B. Trickey

Quantum Theory Project
Physics, Chemistry - University of Florida

trickey@qtp.ufl.edu
www.qtp.ufl.edu/ofdft

Current Topics in Theoretical Chemistry
Quito 2019

Computational Physics and Chemistry– Insight

Numerical Methods for Scientists and Engineers

Richard Wesley Hamming (1915-1998)

2nd Edition, McGraw-Hill, 1973, (1st edition, 1962)

Section 1.1, page 1: "Numerical methods use numbers to simulate mathematical processes, which in turn usually simulate real-world situations. This implies that there is a *purpose* behind the computing. To cite the motto of the book, "The Purpose of Computing is Insight, Not Numbers" .

"This motto is often thought to mean that the numbers from the computing machine should be read and used, but there is much more …. The choice of a particular formula, or algorithm influences not only the computing, but also how we are to understand the results …. *Thus computing is, or at least should be, intimately bound up with both the source of the problem and the use that is going to be made of the answers - it is not a step to be taken in isolation from reality*."

Antecedent: "Nothing is more terrible than activity without insight."
- Thomas Carlyle (1795-1881)

Again from Hamming, ***Numerical Methods for Scientists and Engineers***
2nd Edition, McGraw-Hill, 1973, (1st edition, 1962)

Page 504, the motto
"The Purpose of Computing is Insight, Not Numbers"
is quoted again, ***but with a footnote*****.**

Footnote:
"It is sometimes suggested that the motto be revised to 'the purpose of computing is not yet in sight'."

"…in molecular quantum mechanics, the more accurate the calculations become the more the concepts seem to vanish in thin air."
Robert S. Mulliken, J. Chem. Phys. 43, S2 (1965)

Univ. Florida Free-energy DFT & Orbital-Free DFT Group

Sam Trickey, Jim Dufty

Kai Luo, Daniel Mejía Rodríguez, Jeffrey Wrighton

Affiliates: Frank Harris (U. Utah); Keith Runge (U. Arizona)

Alumni: Lázaro Calderín , Deb Chakraborty, Támas Gál,

Valentin Karasiev, Olga Shukruto, Travis Sjostrom

XC Functional Collaboration (Mexico City):

José Luis Gázquez (UAM- I), Alberto Vela (Cinvestav), Jorge Martín del Campo Ramírez (UNAM), Javier Carmona-Espíndola (UAM-I), Angel M. Albavera Mata (Cinvestav)

***DFT in Magnetic Fields Collaboration*:**

Wuming Zhu (Hangzhou Normal Univ., China)

Funding Acknowledgments:

U.S. Dept. Energy DE-SC 0002129

U.S. Dept. Energy DE-SC 0019330 [Center for Molecular Magnetic Quantum Materials]

U.S. Nat. Science Foundation DMR 1515307

CONACYT (México)

HiPerGator RESEARCH COMPUTING

NERSC National Energy Research Scientific Computing Center

Publications, preprints, & software at http://www.qtp.ufl.edu/ofdft

UF

Motivations -

Fascination

• *PURE* density functional theory - no orbitals, just n(r) – has intrigued me for a long time

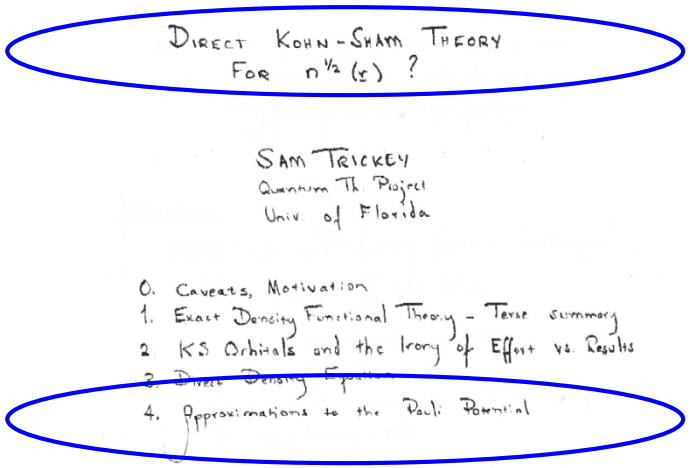
DIRECT KOHN-SHAM THEORY
FOR $n^{1/2}(r)$?

SAM TRICKEY
Quantum Th. Project
Univ of Florida

0. Caveats, Motivation
1. Exact Density Functional Theory - Terse summary
2. K.S. Orbitals and the Irony of Effort vs. Results
3. Direct Density Equations
4. Approximations to the Pauli Potential

Levy and Ou-Yang, Phys. Rev. A 38, 625 (1988) fascinated me. More than two years later I had a chance to think about it while on sabbatical at Max Planck Institut für Astrophysik. These images are from the Institut's Fall 1990 Molecular Physics Seminar collection.

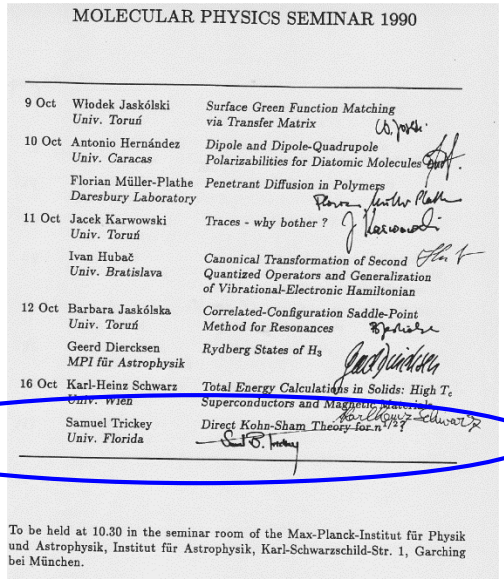
MOLECULAR PHYSICS SEMINAR 1990

9 Oct	Włodek Jaskólski *Univ. Toruń*	*Surface Green Function Matching via Transfer Matrix*
10 Oct	Antonio Hernández *Univ. Caracas*	*Dipole and Dipole-Quadrupole Polarizabilities for Diatomic Molecules*
	Florian Müller-Plathe *Daresbury Laboratory*	*Penetrant Diffusion in Polymers*
11 Oct	Jacek Karwowski *Univ. Toruń*	*Traces - why bother ?*
	Ivan Hubač *Univ. Bratislava*	*Canonical Transformation of Second Quantized Operators and Generalization of Vibrational-Electronic Hamiltonian*
12 Oct	Barbara Jaskólska *Univ. Toruń*	*Correlated-Configuration Saddle-Point Method for Resonances*
	Geerd Diercksen *MPI für Astrophysik*	*Rydberg States of H_3*
16 Oct	Karl-Heinz Schwarz *Univ. Wien*	*Total Energy Calculations in Solids: High T_c Superconductors and Magnetic Materials*
	Samuel Trickey *Univ. Florida*	*Direct Kohn-Sham Theory for $n^{1/2}$?*

To be held at 10.30 in the seminar room of the Max-Planck-Institut für Physik und Astrophysik, Institut für Astrophysik, Karl-Schwarzschild-Str. 1, Garching bei München.

Motivations

Simulation

Warm Dense Matter

- **Challenging region *between* normal condensed matter and plasmas:**
  T < 100eV (≈1,100,000 K) *P* from 0 → thousands of GPa.
- **Inertial confinement fusion pathway; giant planet & exo-planet interiors; shock compression experiments**

Warm Dense Matter Panel, High Energy Density Laboratory Plasma ReNew Workshop; Nov. 2009

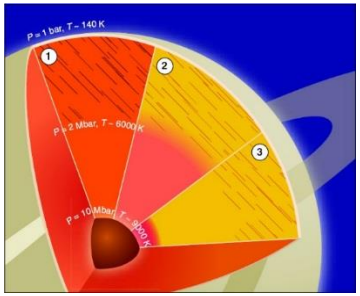

Left: Interior of Saturn [J.J. Fortney, Science 305, 1414 (2004)]:
(1) At an age of ≈ 1.5 billion years
(2) Current Saturn according to previous H-He phase diagram
(3) Current Saturn according to newer evolutionary models

Current best practice to handle materials under such extreme conditions = ab initio Molecular Dynamics (AIMD)

- **Born-Oppenheimer MD**
- **Free-energy DFT for electronic forces (Kohn-Sham solution consumes vast majority of run time)**

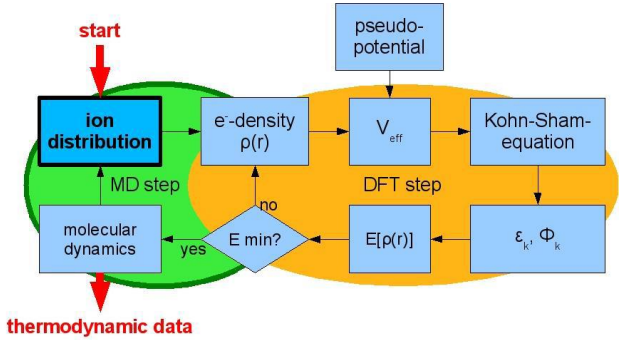

Desiderata for AIMD -

- **Accurate, computationally efficient exchange-correlation (XC) free energy functional**
- **Orbital-free DFT for linear scaling ⇒**
  - **orbital-free non-interacting KE and non-interacting entropy**

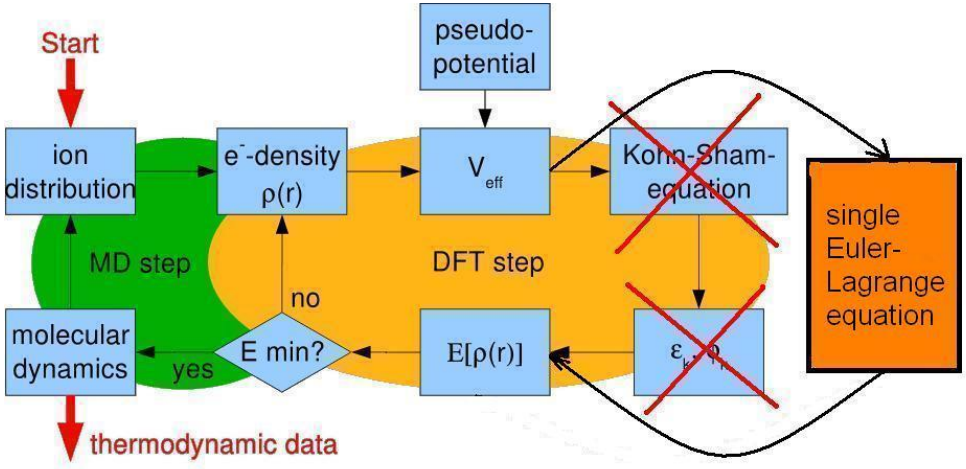

Orbital-free DFT in 2 equations

$$E[n] = \mathcal{T}_s[n] + E_H[n] + E_{xc}[n] + E_{ext}[n]$$

Modified Kohn-Sham equation

$$\frac{\delta E[n]}{\delta n} = \mu$$

Never use the K-S orbitals explicitly.

Desiderata for AIMD -

- **Accurate, computationally efficient exchange-correlation (XC) free energy functional**
- **Orbital-free DFT for linear scaling ⇒**
  - **orbital-free non-interacting KE and non-interacting entropy**
  - **orbital-free XC free energy ⇒**

orbital-free XC energy (ground-state)

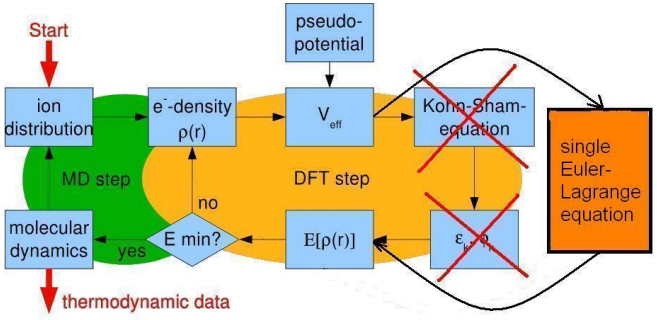

Jacob's Ladder = Perdew-Schmidt pyramid (T=0 K)

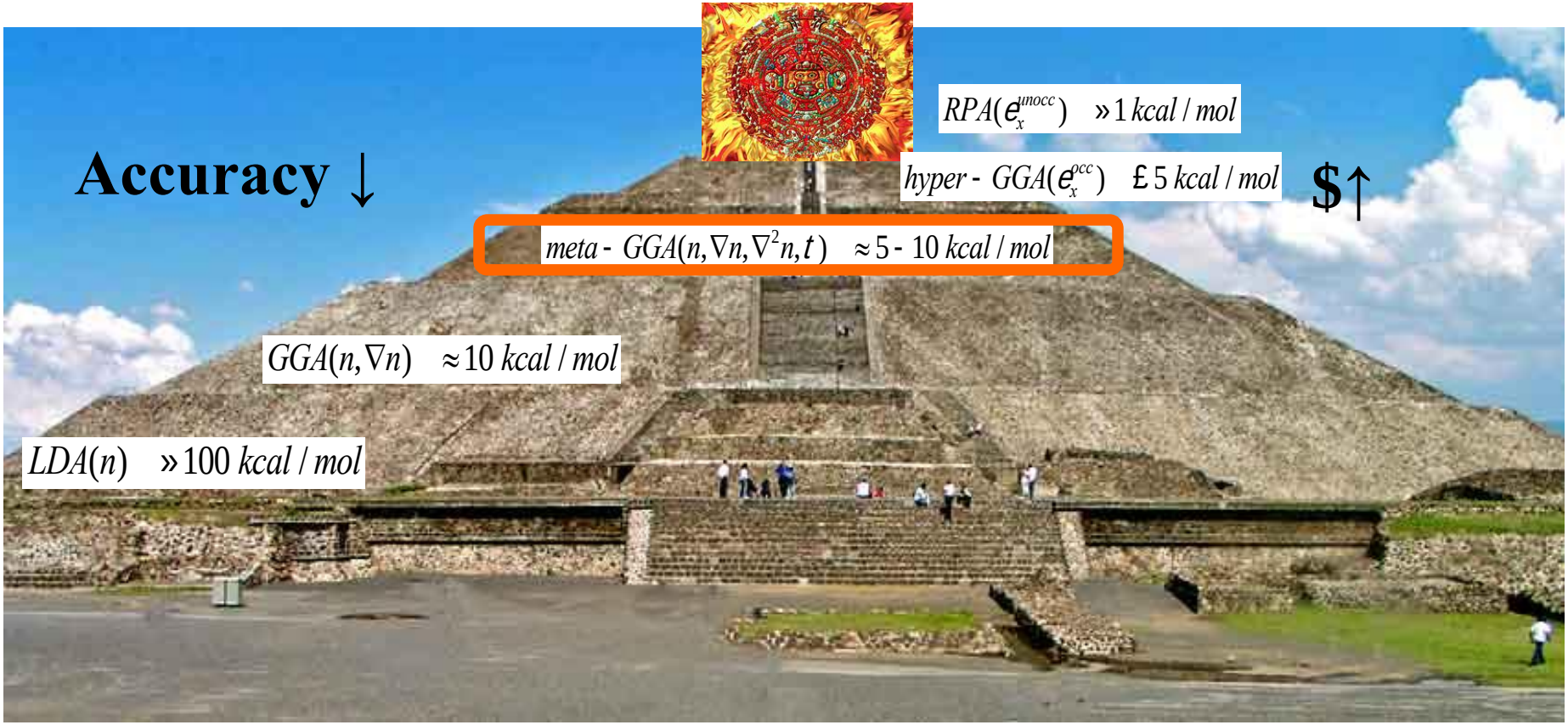

$$E_{XC}[n] = \int d\mathbf{r}\, n(\mathbf{r})\, \varepsilon_X(n)\, F_{XC}(n, \nabla n, \ldots)$$

$$E_x^{XX}\left[\{\phi_i(\mathbf{r})\}\right] = -\frac{1}{2}\sum_{i,j}\left[\int \frac{\phi_i^*(\mathbf{r})\phi_j^*(\mathbf{r}')\phi_j(\mathbf{r})\phi_i(\mathbf{r}')}{|\mathbf{r}-\mathbf{r}'|} d\mathbf{r}d\mathbf{r}'\right]$$

$$\tau := \frac{1}{2}\sum_i |\nabla \varphi_i|^2$$

Borrowed from A. Vela

Kohn-Sham equation versus generalized Kohn-Sham equation -

$$E[n] = \mathcal{T}_s[n] + E_H[n] + E_{xc}[n] + E_{ext}[n]$$

Kohn-Sham equation

$$\frac{\delta E[n]}{\delta n} = \mu \quad \Rightarrow \quad \left\{ -\tfrac{1}{2}\nabla^2 + v_H[n(\mathbf{r})] + v_{xc}[n(\mathbf{r})] + \mathrm{v}_{ext}[n(\mathbf{r})] \right\} \varphi_j(\mathbf{r}_1) = \varepsilon_j \varphi_j(\mathbf{r}_1)$$

No orbital dependence in potentials

Generalized Kohn-Sham equation

$$\frac{\delta E[n]}{\delta \varphi_j} = \mu \quad \Rightarrow \quad \left\{ -\tfrac{1}{2}\nabla^2 + v_H[n(\mathbf{r})] + v_{xc}[\{\varphi(\mathbf{r})\})] + \mathrm{v}_{ext}[n(\mathbf{r})] \right\} \varphi_j(\mathbf{r}_1) = \varepsilon_j \varphi_j(\mathbf{r}_1)$$

Orbital -dependent XC potential if E_{xc} is orbital-dependent

gKS is *not* equivalent to KS for $E_{xc}[\varphi]$ Z-H Yang et al. Phys. Rev. B 93, 205205 (2016)

$$n(\mathbf{r}) = \sum_j f(\varepsilon_j) \left| \varphi_j(\mathbf{r}) \right|^2 \quad ; v_H[n] = \frac{\delta E_H}{\delta n} \quad ; \quad E_H = \frac{1}{2} \int d\mathbf{r}_1 d\mathbf{r}_2 \frac{n(\mathbf{r}_1) n(\mathbf{r}_2)}{|\mathbf{r}_1 - \mathbf{r}_2|}$$

UF

Conventional zero-temperature meta-GGA functionals -

$$E_{xc}[n] = \int d\mathbf{r}\, \varepsilon_{xc}^{ueg}(n)\, F_{xc}\left(n, \nabla n, \tau(\varphi)\right)$$

$$\tau(\varphi[n]) = \frac{1}{2}\sum_i f_i \left|\nabla \varphi_i\right|^2$$

$$T_s[n] = \int d\mathbf{r}\, t(\varphi[n])$$

KS kinetic energy density; Orbital dependence

- PKZB [Phys. Rev. Lett. **82**, 2544 (1999)]
- TPSS [Phys. Rev. Lett. **91**, 146401 (2003)]
- TM [Phys. Rev. Lett. **117**, 073001 (2016)]

$$z := \tau_W / \tau(\varphi)$$

$$\alpha := \frac{\tau(\varphi) - \tau_W}{\tau_{TF}}$$

- TPSS
- MVS [PNAS **112**, 685 (2015)]
- SCAN [Phys. Rev. Lett. **115**, 036402 (2015)]

$$w := \frac{\tau_{TF}/\tau(\varphi) - 1}{\tau_{TF}/\tau(\varphi) + 1}$$

- M06L [J. Chem. Phys. **125**, 194101 (2006)]

GGA kinetic energy density functional

$$E[n] = \mathcal{T}_s[n] + E_H[n] + E_{xc}[n] + E_{ext}[n]$$

Modified Kohn-Sham equation

$$\frac{\delta E[n]}{\delta n} = \mu$$

VT84F – our best GGA kinetic density functional at the time the project started.

$$\mathcal{T}_s^{GGA}[n] = c_{TF} \int d\mathrm{r}\, n^{5/3}(\mathbf{r}) F_t\left(s(\mathbf{r})\right)$$

$$\tau_s^{approx} = c_{TF} n^{5/3} \left(F_\theta^{VT84F} + \frac{5s^2}{3} \right)$$

V.V. Karasiev, D.Chakraborty, O.A. Shukruto and S.B. Trickey, Phys. Rev. B 88, 161108(R) (2013)

VT-84F (T = 0 K) as a deorbitalizer?

Try this

$$\alpha^{approx} := \frac{\tau_s^{approx} - \tau_W}{\tau_{TF}} \qquad \mathcal{T}_s^{GGA}[n] = c_{TF}\int d\mathbf{r}\, n^{5/3}(\mathbf{r}) F_t\left(s(\mathbf{r})\right)$$

$$\tau_s^{approx} = c_{TF} n^{5/3}\left(F_\theta^{VT84F} + \frac{5s^2}{3}\right)$$

Quality measure (initial screening)

$$\sigma = \frac{1}{\mathcal{T}_s}\int dr \left|\tau_s^{orb} - \tau_s^{approx}\right|; \quad \tau_s^{orb} \equiv \tau_s(\varphi)$$

J. Chem. Phys. **127**, 144109 (2007)

Evaluated post-scf on HF densities for first 18 neutral atoms

Exemplifies something basic. A good

$$\mathcal{T}_s^{GGA}[n] = \int d\mathbf{r}\, \tau_s^{approx}$$

doesn't guarantee a good τ_s^{approx} **(Gauge problem).**

TABLE I. Average σ values for the first 18 neutral atoms computed with several kinetic-energy density functionals. "Regularized" denotes conformance with the von Weizsäcker lower bound. Other functionals not referenced in the text also were used, including Tran and Wesolowski (TW02) [49], Lembarki and Chermette (LC94) [50], Ou-Yang and Levy (OL1 and OL2) [51] and Ernzerhof (E00) [52]. Functionals ending in "+L" were built by adding $20/9\,q$ to their original enhancement function.

Functional	Regularized?	σ
PBE2	no	1.576
VT84F	no	1.405
PBE4	no	1.272
LP	no	1.112
APBEK	no	1.028
TW02	no	1.027
LC94	no	1.027
OL2	no	1.017
OL1	no	1.016
GEA2	no	1.013
E00	no	0.996
LP+L	yes	0.827
W	yes	0.473
RDA	yes	0.382
CR	yes	0.271
MVT84F	yes	0.243
TW02+L	yes	0.239
GEA2+L	yes	0.237
MVT84F+L	yes	**0.164**
TFLreg	yes	**0.147**
PC	yes	**0.117**
CRloc	yes	**0.103**

D. Mejía Rodríguez and S.B.T.; Phys. Rev. A 96, 052512 (2017)

Reparametrize α directly

Quality measures

$$\delta_\alpha := \frac{1}{N_{systems}} \int d\mathbf{r} n(\mathbf{r}) \left| \alpha^{orb} - \alpha^{approx} \right|$$

J. Chem. Phys. **146**, 064105 (2015)

$$\delta_\alpha^{near} := \frac{4\pi}{N_{systems}} \int_0^4 dr r^2 n(\mathbf{r}) \left| \alpha^{orb} - \alpha^{approx} \right|$$

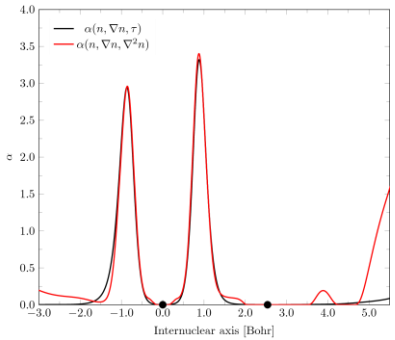

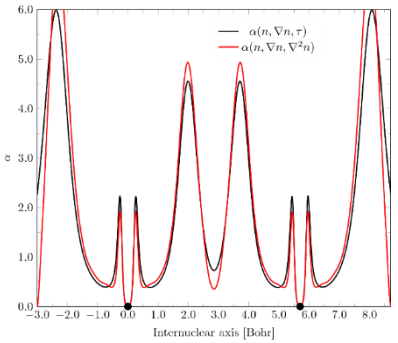

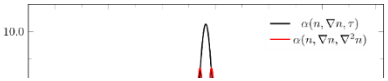

Again, evaluated post-scf on HF densities for first 18 neutral atoms

TABLE III. Error indicator $\Delta_\alpha + \Delta_\alpha^{\text{near}}$ values for the reoptimized mGGA$\{a,b\}$ kinetic-energy density-functional approximations.

	a	b	$\Delta_\alpha + \Delta_\alpha^{\text{near}}$
PC	0.538900	3.000000	0.712057
PCopt	1.784720	0.258304	0.649567
CRloc	−0.275000	2.895000	0.631376
TFLreg	0.000000	2.222222	0.398936
CRopt	−0.295491	2.615740	0.383805
TANH	−0.216872	2.528000	0.365022
TFLopt	−0.203519	2.513880	0.361805

D. Mejía Rodríguez and S.B.T.;
Phys. Rev. A 96, 052512 (2017)

Deorbitalize meta-GGA made very simple ("MVS")

$$E_{xc}[n] = \int d\mathbf{r}\, \varepsilon_{xc}^{HEG}(n)\, F_{xc}\left(n, \nabla n, \tau(\varphi)\right)$$

$$F_x^{MVS}(s,\alpha) = \frac{1 + 0.174\, f_x(\alpha)}{(1 + 0.0233 s^4)^{1/8}}; \qquad f_x(\alpha) = \frac{1-\alpha}{\left[(1-1.6665\alpha^2)^2 + 0.7438\alpha^4\right]^{1/4}}$$

Mean absolute deviations (MAD)

	Original	PCopt	CRopt
Heats of formation (kcal/mol)	18.34	15.94	6.20
Bond Lengths (Å)	0.0139	0.013	0.0130
Frequencies (cm^{-1})	52.0	46.0	42.6

Surprise! Best-performing deorbitalization; superior to original.

Gratifying result: faithful deorbitalization resembles MAD of original nicely

D. Mejía Rodríguez and S.B.T.;
Phys. Rev. A 96, 052512 (2017)

Deorbitalize SCAN

$$E_{xc}[n] = \int d\mathbf{r}\, \varepsilon_{xc}^{HEG}(n)\, F_{xc}\left(n, \nabla n, \tau(\varphi)\right)$$

$$F_x^{scan}(s,\alpha) = \left\{ h_x^1(s,\alpha) + f_x(\alpha)\left[1.174 - h_x^1(s,\alpha)\right]\right\} g_x(s)$$

$$g_x(s) = 1 - e^{-a_1/\sqrt{s}}$$

$$f_x(\alpha) = e^{-c_{1x}\alpha/(1-\alpha)}\theta(1-\alpha) - d_x e^{c_{2x}/(1-\alpha)}\theta(\alpha - 1)$$

$h_x^1(s,\alpha)$ is an approximate resummation of the fourth-order gradient expansion for exchange

$\theta(x)$ is the Heaviside unit step function

At right: plots of F_{xc} for SCAN (black) and SCAN-L (red) for H and Ar atoms; SCAN-L done with PCopt deorbitalization

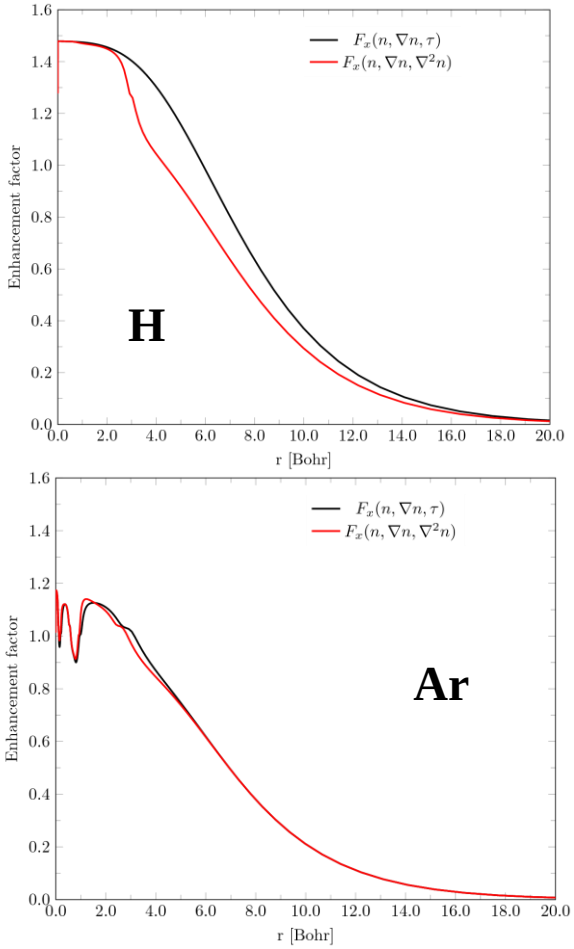

D. Mejía Rodríguez and S.B.T.;
Phys. Rev. A 96, 052512 (2017)

Original SCAN vs. SCAN-L: molecular benchmark

		SCAN	SCAN-L
Heats of formation G3 Set [kcal/mol]	**ME**	**-3.62**	**2.11**
	MAE	**5.12**	**5.67**
Bond distances T96R [Å]	**ME**	**0.0035**	**0.0073**
	MAE	**0.0089**	**0.0105**
Vibrational frequencies T82F [cm^{-1}]	**ME**	**15.3**	**-11.7**
	MAE	**31.9**	**28.7**

SCAN-L performs essentially as well as SCAN for these standard molecular tests.

Convergence of both SCF and geometry optimization are stable.

D. Mejía Rodríguez and S.B.T.;
Phys. Rev. A 96, 052512 (2017)

Original SCAN vs. SCAN-L: crystalline benchmark

		SCAN	SCAN-L
Lattice constants [Å]	**ME**	**0.011**	**0.009**
	MAE	**0.025**	**0.024**
	MARE(%)	**0.53**	**0.55**
Bulk moduli [GPa]	**ME**	**3.0**	**-3.0**
	MAE	**6.9**	**9.2**
	MARE(%)	**7.1**	**9.4**
Cohesive energies [eV/atom]	**ME**	**-0.01**	**-0.017**
	MAE	**0.24**	**0.26**
	MARE(%)	**5.93**	**6.42**
KS Band gaps [eV]	**ME**	**-1.26**	**-1.58**
	MAE	**1.26**	**1.58**

VASP with PBE PAWs

SCAN-L performs as well as SCAN for 57 solids.

SAME deorbitalization for solids *and* molecules.

SCF convergence for SCAN-L is same or faster than SCAN

Overall SCAN-L speed in VASP is 3 times faster than SCAN.

Band gap difference reflects difference between gKS (SCAN) and KS (SCAN-L)

D. Mejía Rodríguez and S.B.T.;
Phys. Rev. B 98, 115161 (2018)

Original SCAN vs. SCAN-L: crystalline benchmark

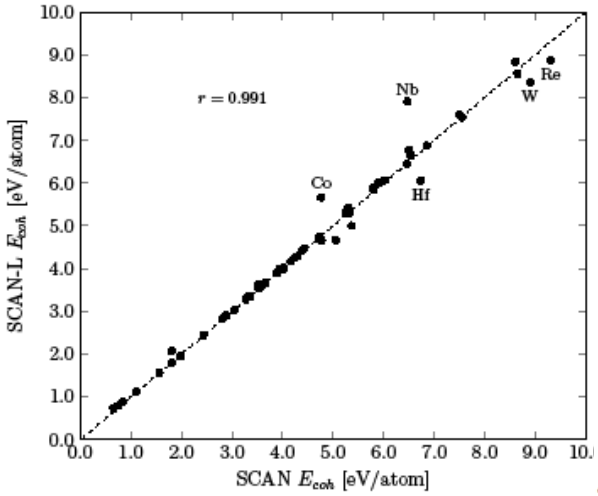

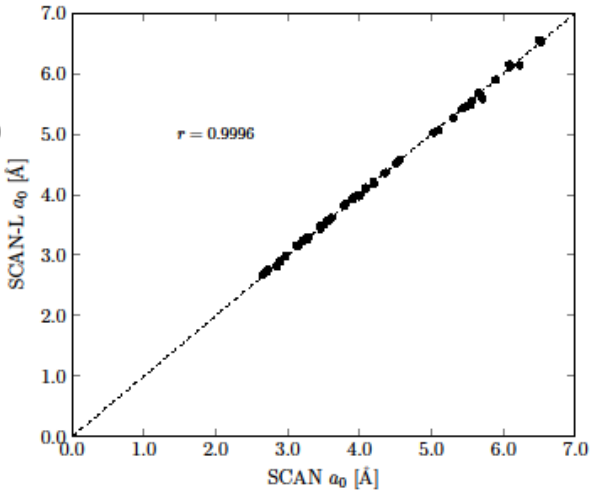

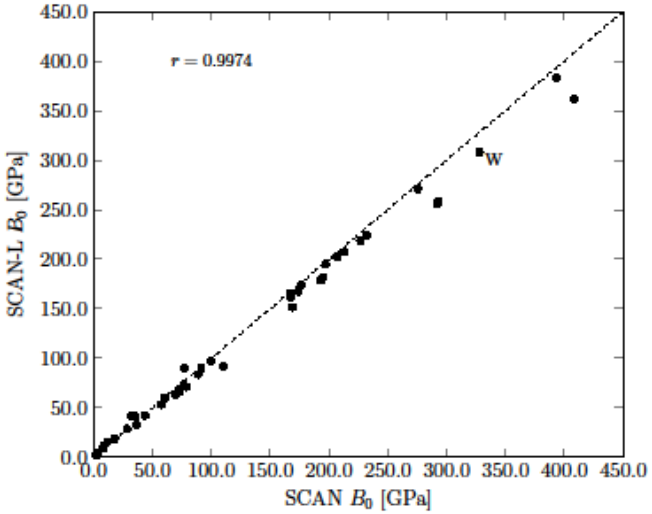

D. Mejía Rodríguez and S.B.T.;
Phys. Rev. B 98, 115161 (2018)

Original SCAN vs. SCAN-L: Graphene bilayer interlayer binding

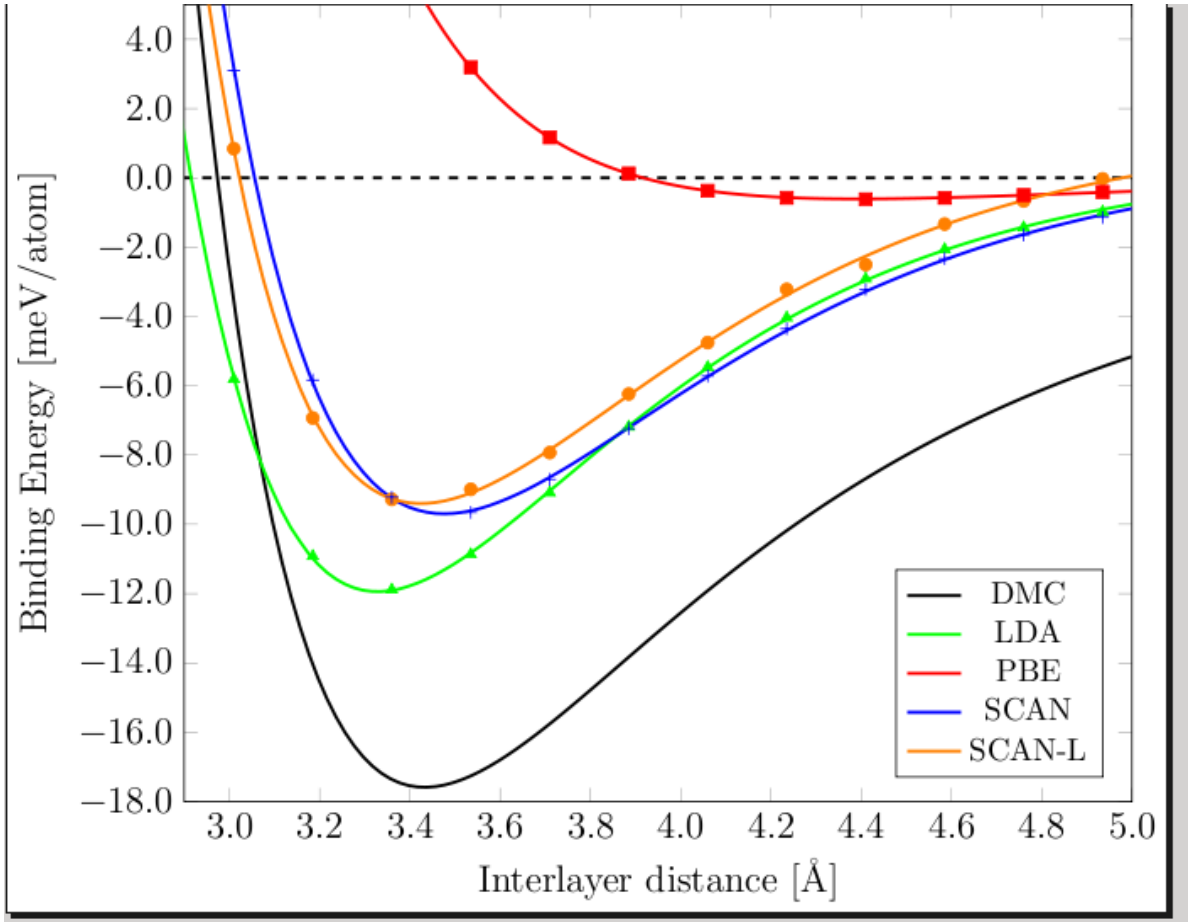

D. Mejía Rodríguez and S.B.T.;
Phys. Rev. B 98, 115161 (2018)

DMC data: Phys. Rev. Lett. **115**, 115501 (2015)

VASP timings

TABLE VII. Comparative timings for PBE, SCAN, and SCAN-L calculations in the original and modified mGGA and GGA trunks of VASP. All times in seconds. See text for trunk labels.

XC	Trunk	Original Code	Modified Code
PBE	GGA=PE	12.38	12.85
PBE	METAGGA=PBE	36.75	37.57
SCAN	METAGGA=SCAN	61.28	–
SCAN-L	GGA=SL	–	19.32
SCAN-L	METAGGA=SCANL	–	50.72

D. Mejía Rodríguez and S.B.T.;
Phys. Rev. B 98, 115161 (2018)

Constraint-based parametrization is delicate

Regularized SCAN functional

Cite as: J. Chem. Phys. 150, 161101 (2019); doi: 10.1063/1.5094646
Submitted: 4 March 2019 • Accepted: 8 April 2019 •
Published Online: 29 April 2019

Albert P. Bartók[1,a] and Jonathan R. Yates[2]

TABLE III. Equilibrium lattice constants (Å) of a selection of metallic and semiconductor solids (a subset of "LC20" in Ref. 20), computed using the rSCAN functional. Experimental values, corrected for zero point anharmonic expansion, were taken from Ref. 30, and reference SCAN values from Ref. 20.

	Li	Na	Ag	C	Si	SiC	LiF	MgO
Expt.	3.451	4.207	4.063	3.555	5.422	4.348	3.974	4.188
SCAN	3.460	4.190	4.079	3.550	5.424	4.349	3.980	4.206
rSCAN	3.453	4.197	4.039	3.555	5.441	4.353	3.964	4.200

"We propose modifications to the [SCAN] functional … to eliminate numerical instabilities. …The regularized SCAN is designed to match the original form very closely and we show that its performance remains comparable."

TABLE IV. Dissociation energies (meV/monomer) of a few low-energy water hexamers conformations, the equilibrium bond length (Å), bond angle, and dipole moment (Debye) of the water molecule. Reference hexamer dissociation values are computed by CCSD(T),[31] while the geometry of the water molecule is from Ref. 32 and its dipole moment from Ref. 33. SCAN values were obtained from Ref. 4.

	Prism	Cage	Book	Chair	r_{OH}	θ_{HOH} (deg)	μ
Ref.	348	346	339	332	0.957	104.5	1.855
SCAN	377	376	370	360	0.961	104.5	1.847
rSCAN	359	358	356	348	0.959	104.4	1.847

UF

Close but not identical (molecules)

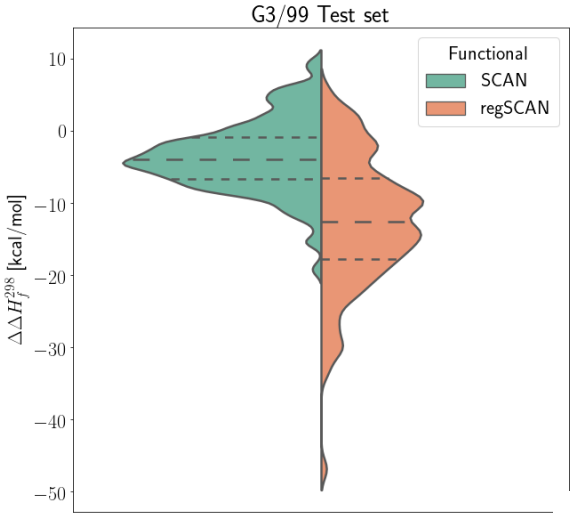

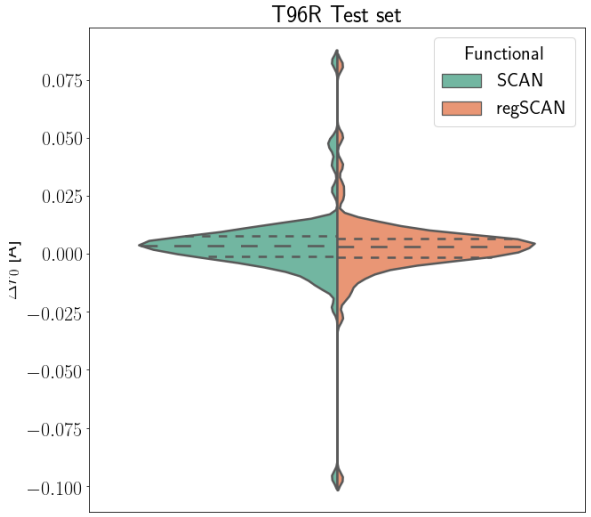

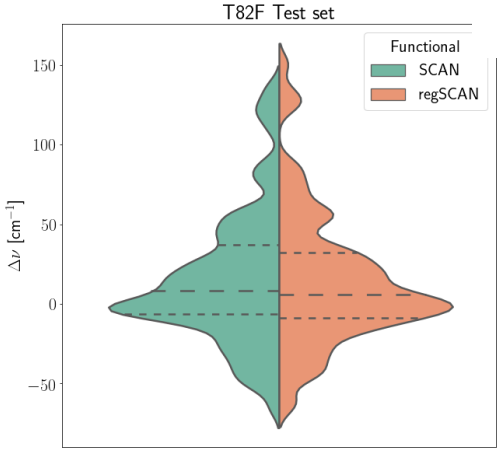

NWChem calcs

g3: heats of formation

t96r: bond lengths

t82f: harmonic vibr. freqs.

D. Mejía Rodríguez, unpublished

Close but not identical (solids)

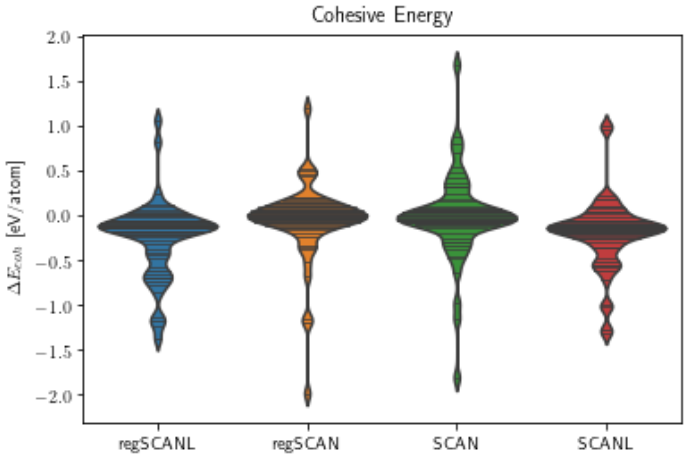

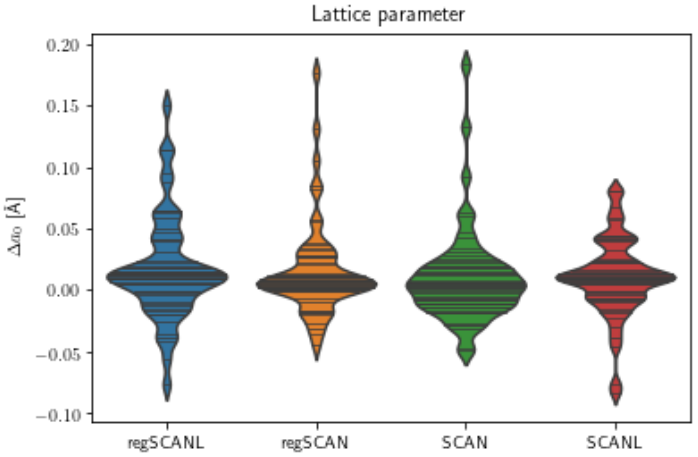

VASP calcs on 55 solids

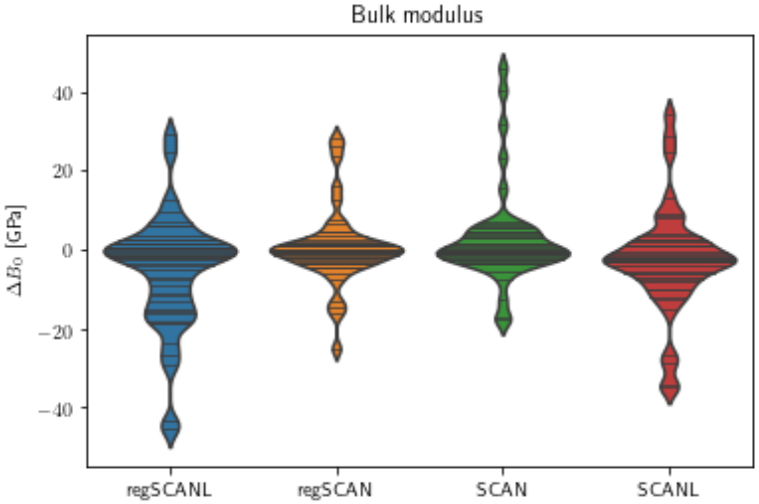

D. Mejía Rodríguez, unpublished

SCAN form is sensitive to technique

SCAN and regSCAN can be sensitive to VASP PAW hardness.

Atomization energies (eV) for three PAW families [VASP 5.4.4)

All-electron values are from NWChem with def2-qzvpp basis

	CO		CO_2		ClF_3		CF_4	
Functional	SCAN	reg SCAN	SCAN	reg SCAN	SCAN	reg SCAN	SCAN	reg SCAN
Default PAW	10.83	11.04	16.63	17.04	6.11	6.22	20.46	20.75
Hard PAW	11.01	11.20	16.98	17.33	5.97	6.26	20.70	21.14
GW PAW	11.04	11.23	17.02	17.38	6.12	6.32	20.89	21.26
All-electron	11.03	11.22	17.02	17.37	6.03	6.29	20.85	21.23

D. Mejía Rodríguez, unpublished

SCAN is more sensitive to grids than regSCAN

SCAN and regSCAN results NWChem with def2-tzvpp basis

MADs for COARSE, MEDIUM, & FINE grids relative to XFINE

	Δf kcal/mol		a_0 Å		υ cm^{-1}	
Functional	**SCAN**	**reg SCAN**	**SCAN**	**reg SCAN**	**SCAN**	**reg SCAN**
COARSE	5.93	0.42	0.001	0.000	25.2	6.0
MEDIUM	2.38	0.09	0.001	0.000	18.4	1.7
FINE	0.77	0.01	0.001	0.000	10.4	0.5

D. Mejía Rodríguez, unpublished

A SCAN limitation

Applicability of the Strongly Constrained and Appropriately Normed Density Functional to Transition Metal Magnetism

Yuaho Fu and David J. Singh

Phys. Rev. Lett. 121, 207201 (2018)

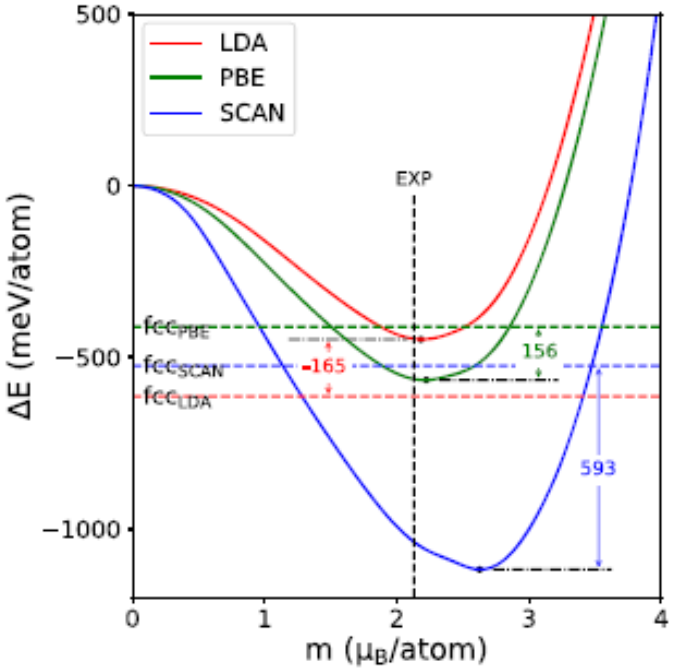

FIG. 1. FSM energy for bcc Fe at the experimental lattice constant of 2.86 Å, on a per atom basis. The dashed lines are the energies of non-spin-polarized fcc Fe, at the optimized lattice parameter for the different functionals. The small dots indicate the minimum energy points.

Also found slightly earlier in:

- E. B. Isaacs and C. Wolverton, Phys. Rev. Mat. 2, 063801 (2018)
- S. Jana, A. Patra, and P. Samal, J. Chem. Phys. 149, 044120 (2018)
- A. H. Romero and M. J. Verstraete, Eur. Phys. J. B 91, 193 (2018).
- M. Ekholm, D. Gambino, H.J.M. Jönsson, F. Tasnádi, B. Alling, and I.A. Abrikosov, Phys. Rev. B 98, 094413 (2018).

A SCAN limitation that doesn't occur in SCAN-L

Applicability of the Strongly Constrained and Appropriately Normed Density Functional to Transition Metal Magnetism

Yuaho Fu and David J. Singh

Phys. Rev. Lett. 121, 207201 (2018)

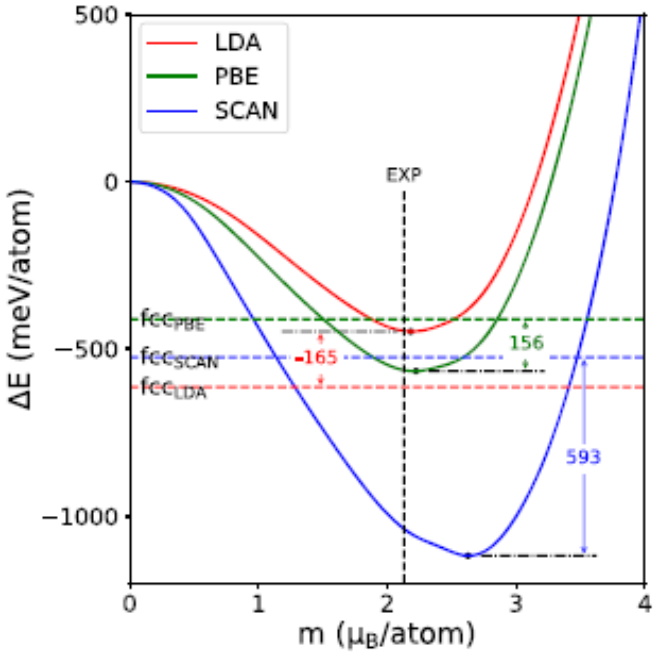

FIG. 1. FSM energy for bcc Fe at the experimental lattice constant of 2.86 Å, on a per atom basis. The dashed lines are the energies of non-spin-polarized fcc Fe, at the optimized lattice parameter for the different functionals. The small dots indicate the minimum energy points.

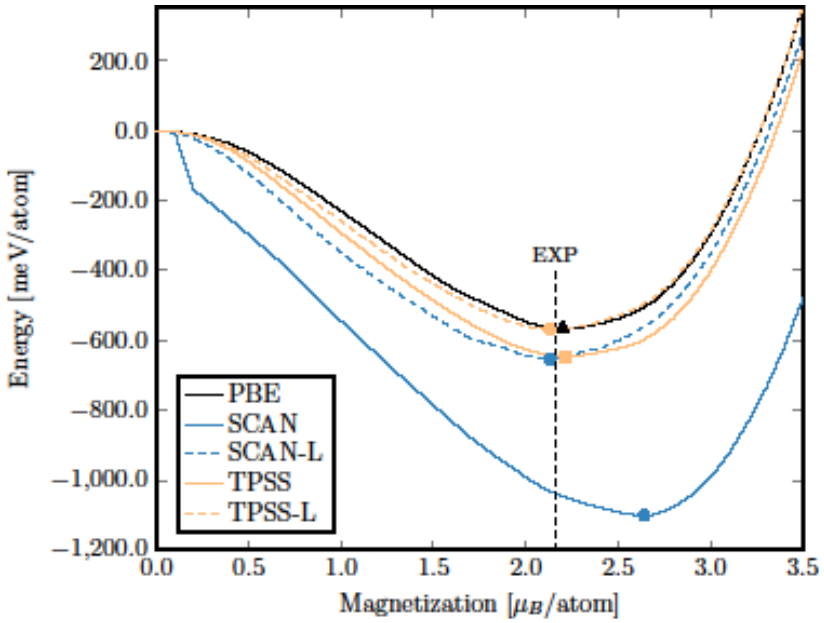

D. Mejía Rodríguez and S.B.T.;
arXiv 1905.01292

SCAN-L differs from SCAN for other transition metals

TABLE II. Co, Ni and V calculated saturation magnetizations and FSM energies for various XC functionals at a_{exp}.

	m_{sp} (μ_B/atom)	E_{mag} (meV/atom)	
hcp Co			
PBE	1.65	-255	
SCAN	1.80	-578	**Magnitude too large**
SCAN-L	1.63	-277	
fcc Ni			
PBE	0.65	-60	
SCAN	0.78	-137	**Magnitude too large**
SCAN-L	0.67	-74	
bcc V			
PBE	0.00	0	
SCAN	0.57	-6	**Wrong; non magnetic**
SCAN-L	0.00	0	

D. Mejía Rodríguez and S.B.T.;
arXiv 1905.01292

SCAN-L differs from SCAN magnetization

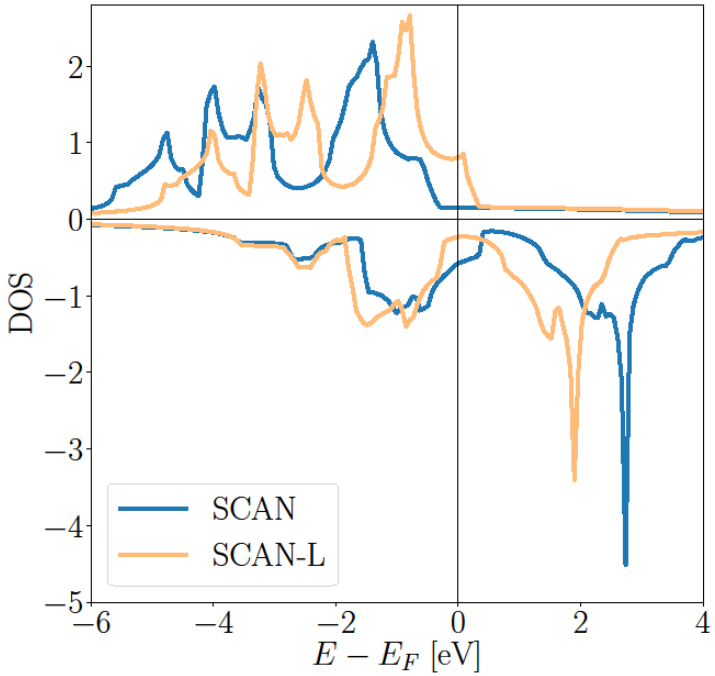

SCAN and SCAN-L density of states, bcc Fe.
Up spin above, down spin below

D. Mejía Rodríguez and S.B.T.;
arXiv 1905.01292

SCAN-L differs from SCAN magnetization

- **Difference doesn't come from PBE PAWs; post SCF calculations with WIEN2K and PBE input density also manifest the difference.**
- **Difference doesn't come from gKS (SCAN) versus KS (SCAN-L); TPSS (gKS) and TPSS-L (KS) don't display such a large difference.**

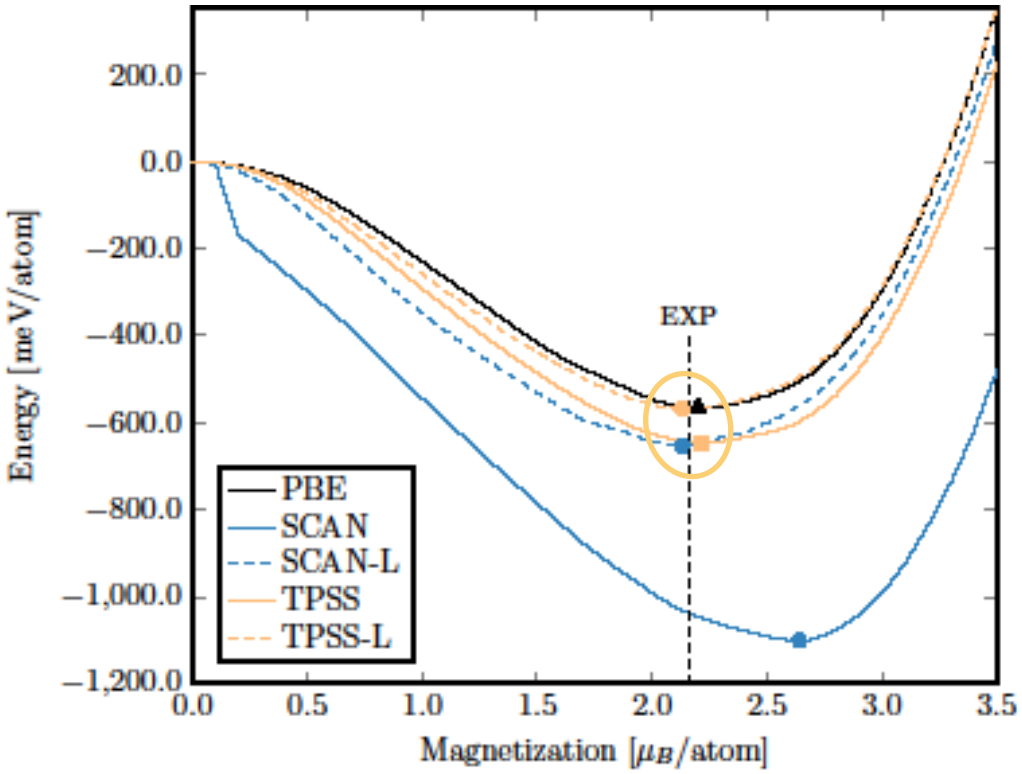

D. Mejía Rodríguez and S.B.T.; arXiv 1905.01292

SCAN-L differs from SCAN magnetization

- **Difference doesn't come from PBE PAWs; post SCF calculations with WIEN2K and PBE input density also manifest the difference.**
- **Difference doesn't come from gKS (SCAN) versus KS (SCAN-L); TPSS (gKS) and TPSS-L (KS) don't display such a large difference.**
- **SCAN-L generates a different (smaller) α from SCAN, especially below r ≈ 1 bohr**
- **SCAN switching function slightly too sensitive in that region and not sensitive enough for > 1 bohr.**
- **regSCAN doesn't fix it.**

TABLE I. Calculated bcc Fe lattice parameters, saturation magnetizations, and FSM energies for various XC functionals at a_{calc}.

	a_{calc} (Å)	m_{sp} (μ_B/atom)	E_{mag} (meV/atom)
PBE	2.82	2.14	-564
TPSS	2.80	2.12	-645
SCAN	2.85	2.60	-1100
regSCAN	2.84	2.62	-1201
SCAN-L	2.81	2.05	-653
TPSS-L	2.81	2.09	-568

D. Mejía Rodríguez and S.B.T.;
arXiv 1905.01292

Summary

*** SCAN-L = de-orbitalized SCAN makes modern mGGA XC functional useful for orbital-free calculations**

*** *SAME* de-orbitalization for *both* solids *and* molecules**

*** SCAN-L via GGA trunk in VASP is 3 times faster than SCAN**

*** SCAN-L available in NWChem (6.8.1) ; soon to be submitted to QuantumEspresso (6.3); will be in VASP , deMon2K, and PROFESS**

*** SCAN-L patches available for VASP 5.4.4, deMon2K 6.05, and PROFESS 3.0 (but we cannot be a help desk!)**

*** SCAN-L and SCAN are *INEQUIVALENT* for transition metal magnetism; motivates improvement or refinement of SCAN switching function**

*** regSCAN is *not* equivalent with SCAN**

*** But both have peculiar sensitivity to PAW hardness.**

*** De-orbitalization renews motivation for studying Laplacian-dependent XC functionals (one de-orbitalized version of MVS is better than original)**

Publications and Downloads - www.qtp.ufl.edu/ofdft